B. Solf

D. Wagner

# Rapid, Precise, Computer-controlled Measurement of X-Y Coordinates

Abstract: An experimental x-y measurement system is described that was designed for the high-speed, high-precision measurements required in integrated circuit manufacturing and for optical measurement applications in which a sufficiently large data base is required for statistical process analysis. The technology for this experimental system differs considerably from that of conventional optical measuring systems in current use and utilizes a computer for data acquisition, manipulation and evaluation. The system, utilizing the edge detection principle, presently operates at a measuring speed of 2.5 cm/s. An analysis gives both the short-term and the long-term precision of the system. The standard deviation for the short-term precision is 0.038  $\mu$ m.

#### Introduction

Precise measurement techniques are required in the manufacture of integrated circuits, in which active and passive elements and their interconnections form two-dimensional patterns of various shapes and sizes. The pattern mask itself, either a photographic emulsion or a thin chrome layer, is generated as an opaque structure on a transparent glass substrate. In the photolithographic process the mask pattern is transferred in several steps to the surface of a silicon wafer, the latter being coated with a photoresist material. Various optical techniques, such as contact or projection printing, may be used for the pattern transfer.

Pattern dimensions and overlay registration become more critical as circuit density increases and pattern size decreases. Product tolerances in the micrometer range are now specified in many process steps. Submicrometer tolerances are required for the masks themselves in order to obtain the product specifications.

The semiconductor manufacturing process depends on a large number of parameters, some of which are not well defined. An evaluation of the semiconductor product, therefore, has to be done on a statistical basis, requiring that conclusions be drawn from a sufficiently large data base. To obtain such a data base, a large number of precise and reliable measurements can be made on masks and wafers by the high-speed process described in this paper.

Measurements of integrated circuit geometries are usually carried out using manually operated instruments, e.g., with optical microscopes. Two- or three-coordinate measuring machines that do not depend on operator precision have been developed by a number of manufacturers. In many cases these machines have evolved from precision machine tools. In turn, they are used mostly for the measurement of machine-tool fabricated parts. The essentials of this technology have recently been described by Young [1]. A very high standard in twocoordinate measurement and control has been achieved in the field of diffraction-grating ruling machines [2, 3]. Automatic calibration of precision scales is performed by a single-axis measuring system described by Hock and Heinecke [4a], and a machine-tool measurement technique was reported by Radio et al. [4b].

High speed and high precision are adverse to each other in all optical measurement systems that rely on the accuracy of the object carrier. The conventional approach to this problem in modern measuring systems has been to aim for high precision by using very precise mechanical guide rails in the object carrier. These carriers are usually very heavy and slow.

The techniques used in the experimental system described here offer both the speed and the precision to provide the large number of optical measurements needed for statistical evaluation.

## Measurement system

## · Philosophy of high-speed measurement

Many parameters that influence the precision of a measuring system vary slowly with time. Among these are environmental changes, mechanical deformations due to temperature drift, etc. Their influence can be suppressed by considerably reducing the measurement time interval. However, high-speed measurements require a new approach in the design of the measuring equipment. First, the contradiction between speed and precision that exists in present measuring systems can be reduced by using an on-line, two-dimensional measuring technique to determine continuously the object position and to operate the measuring system according to the Abbé comparator principle [5]. The latter eliminates measurement errors of the first order and thereby gives the required precision with a less accurate, and therefore lighter and faster, object carrier. Second, the response time of the edge detection device must be of the order of a microsecond, if the geometries are to be located reliably with rapid, continuous tracing. An electro-optic device has been developed that serves this purpose.

In addition, an on-line computer has to be an integral part of the system [6]. For a system for measuring integrated circuits this is particularly important in view of the quantity of data to be handled. The computer provides three basic functions: control of the entire measuring process, data acquisition, and data evaluation and reporting.

Among the data evaluation programs used, the one for mean value calculation from repeated measurements is of particular significance. This shows how the data processor can help to improve the effective measuring precision. From a statistical point of view the factor of improvement is equal to the square root of the number of repetitions. Thus the combination of high-speed instrumentation with an on-line computer provides the basis for accepting repeated measurements as a standard procedure.

# • System configuration

The experimental setup of the two-dimensional measuring system is indicated in the block diagram in Fig. 1. An x-y table, lead-screw-driven by two stepping motors, serves as the carrier of the measured object. A He-Ne laser is used for the x- and y-interferometers, and is set up as the on-line table-position measuring system. The movable mirrors are mounted on the x-y table in a com-

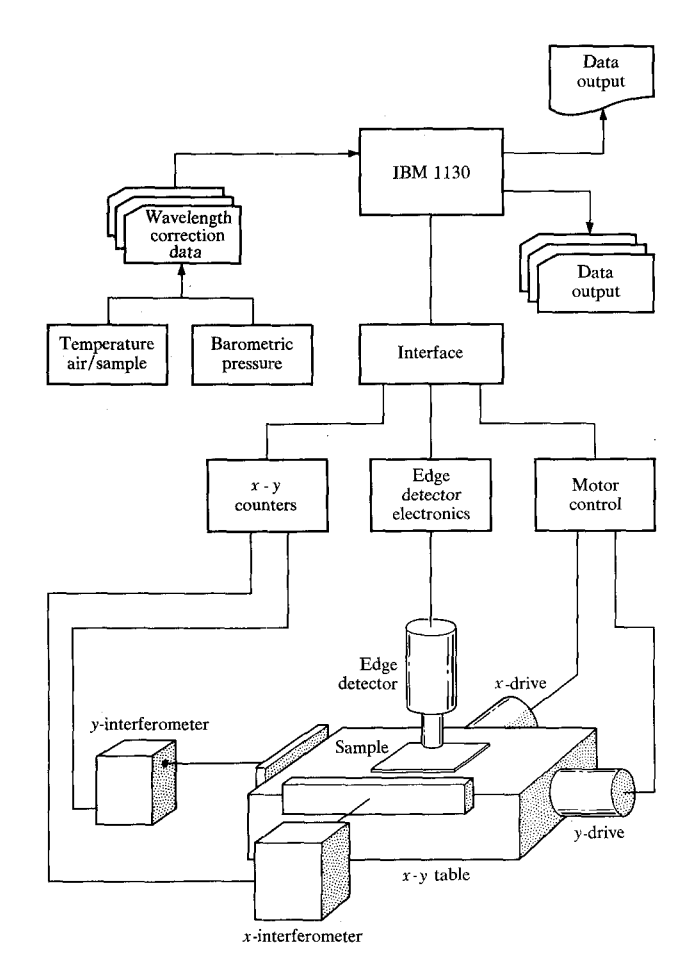


Figure 1 Block diagram of high-precision measuring system.

mon plane with the measured object. An edge detection system is mounted stationary over the x-y table. This system detects the pattern edges passing its optical axis.

The actual measurement is performed "on the fly" by relating the pattern geometry to the table-position measurement system. The table position is continuously monitored by the x- and y-interferometer counters, and the two coordinates of the pattern edge can be read from these counters. The reading is initiated when the edge of a pattern reaches the optic axis of the edge detection system.

The table movement is controlled by an IBM 1130 computer which is programmed according to the measuring plan. Measurement is usually done in a scanning mode. Single scans as well as meander-type scanning can be performed. The x-y table is started from a home position, is moved to the start position of the first measurement scan, and begins to scan from there. All coordinate data required for these table movements are provided by the computer.

The computer also serves as a data acquisition system, the pattern coordinates being collected as provided

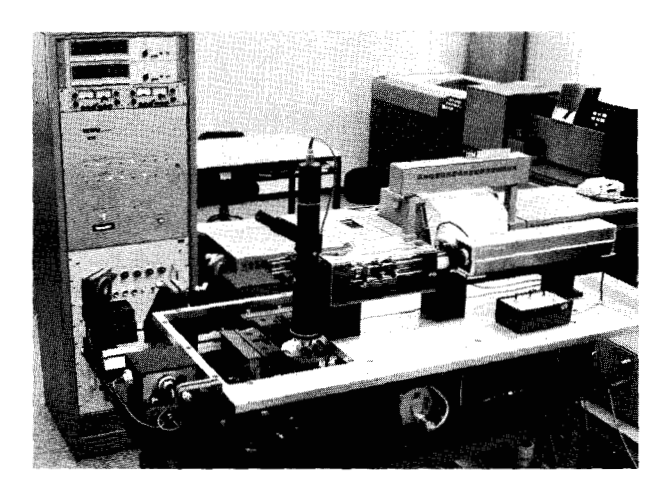


Figure 2 X-Y measuring system.

by the position measuring equipment in connection with the edge detection system. The total measuring system is connected to the computer through a specially designed interface. This interface modifies the in- and outgoing data and the data formats, and also provides some control functions.

Since changes in environmental parameters affect the measurement precision, the data for air and object temperatures and for air pressure are recorded and fed into the computer by punch cards. These data are used to correct the actual measurement values. However, these and additional data manipulations are carried out after completion of the measurement.

Figure 2 is a photograph of the experimental system with the 1130 computer in the background. The interface is mounted in the cabinet on the left side, which also contains the two interferometer counters and the two motor control units. The measurement system in the front shows the x-interferometer evaluation unit, the x-y table with the two interferometer mirrors, and the measurement object. Mounted on a platform over the table is the edge detection system.

A more detailed description of the various components of the system is given in the paragraphs following.

## • X-Y transport and coordinate measuring system

The basis for the transport mechanism is a precision x-y table, weighing 22 kg, and having a 10 cm  $\times$  10 cm traverse driven by stepping motors by means of lead screws. In the main measuring direction the table runs typically at 2.5 cm/s, a speed that can be used for a long period of time without excessive wear of the lead-screw mechanism. Smooth and vibration-free start-and-stop is provided by a special circuit in the table control electronics.

The x-y stage carries the plate holder, which is a precision-ground vacuum chuck that clamps the target plate over the major part of its back surface. Means are provided for angular fine adjustment of the chuck around the vertical axis. This adjustment is needed to obtain parallelism between coordinate axes of the target and the x-y stage. In addition, the chuck can be leveled. This feature is required at times to keep the target surface within the limits of the dynamic focus range of the edge detector and to eliminate measurement errors due to target inclination.

The instantaneous position of the upper stage of the x-y table is tracked by a dual-axis laser interferometer. The concept of this system is such that 1) the beam geometry is in accordance with Abbé's comparator principle for both axes, and 2) x- and y-coordinates are measured independently with reference to the machine base.

At the time when the development of the present system started, true dual-axis interferometers existed only in a small number of development laboratories. Since then, this type has become commercially available. The majority of interferometric x-y measurement installations, however, use essentially two single-axis interferometers that substitute for conventional glass scale or calibrated lead-screw systems. But this arrangement does not obey the Abbé condition and is thus prone to measurement errors due to mechanical imperfections in the system, such as squareness error or nonlinear travel of the x-y table. As a consequence, these systems are usually built on the basis of bulky, slow moving two-coordinate tables with high inherent mechanical precision

According to the Abbé principle, the influence of table guidance errors on measurement precision is eliminated in first approximation, provided the dimension to be measured extends along one axis with the length scale used [5]. Applied to interferometric length measurement, this means that the dimension to be measured should be collinear with the target beam of the interferometer. The interferometric technique is also the convenient way to implement the comparator principle in the two-dimensional case. Accordingly, the two mutually perpendicular target beams of a dual-axis interferometer are in-plane with the measurement object, and the beam axes intersect under the measurement head.

The present system is designed in accordance with this geometry. The x and y interferometers have the standard geometry of Michelson's interferometer, using plane mirrors both as fixed reference reflectors and as target reflectors. The target reflectors, mounted on the upper platform of the x-y table, have a length sufficient that the table can be exercised over the full range of its x(y)-axis without interfering with the operation of

the y(x)-axis interferometer. The flatness of these mirrors is specified to  $\lambda/20 \ (\approx 0.03 \ \mu m)$ . A light source common to both interferometers is a Lamb-dip stabilized He-Ne laser. The quadrature signals required for the reversible counting of the interferometer fringes are generated by using circular polarization [7]. The symmetric output signal oscillates around a mean value of zero, rendering the length increment, equivalent to each fringe count, independent of fringe contrast variations. The original optical resolution of the interferometers is  $\lambda/2$  but is improved to  $\lambda/8 \ (\approx 0.08 \ \mu m)$  per digit through further electronic interpolation in the reversible counters.

# • Edge detection head

Leading and trailing edges of the geometries subject to measurement are localized by the edge detection head. Mounted on a bridge-like construction above the x-y table, this unit is in rigid connection with the machine base. The precision and speed of the edge detector have to be compatible with those of the interferometer and x-y table, i.e., the  $2\sigma$ -limit of the precision should not exceed a fraction of the interferometer resolution  $(0.08 \ \mu m)$ . The response time should be short enough to permit operation "on the fly" at the table speed of typically  $2.5 \ cm/s$ .

These requirements are met by a recently developed instrument [8, 9] using laser illumination and electro-optic light beam deflection. The use of coherent light permits the target to be probed by an intense microphotometric light spot of a diameter that is nearly diffraction limited. This spot is periodically deflected at a submicrometer amplitude. Small spot size and dynamic probing together form the basis for obtaining high precision. A short response time is achieved by using high-frequency oscillations that are easily generated by electro-optical means.

The optical setup of the instrument and the essential numerical data are given in Fig. 3. Figure 4 shows schematically the signal processing. A detailed description of the operating principle has been given elsewhere [8, 9]. On chrome masks the edge detection precision ( $2\sigma$  limit) is below 0.03  $\mu$ m at 2.5 cm/s table speed. This value includes the uncertainties in locating both ends of the measured interval. The minimum dimension that can be measured without mutual interference of the edge signals due to the light spot size is about  $2 \mu$ m. Sensitivity in two dimensions is obtained by orienting the light spot deflection at 45° with respect to the table axes.

Precision, unfortunately, is obtained at the expense of depth of focus. With the present unit the effective depth of focus is not greater than  $\pm 1~\mu m$ . Therefore, care has to be taken that the working distance of the lens be maintained within this limit during operation. The surface waviness of integrated circuit masks usually far exceeds this limit. For this reason, the edge detector is equipped

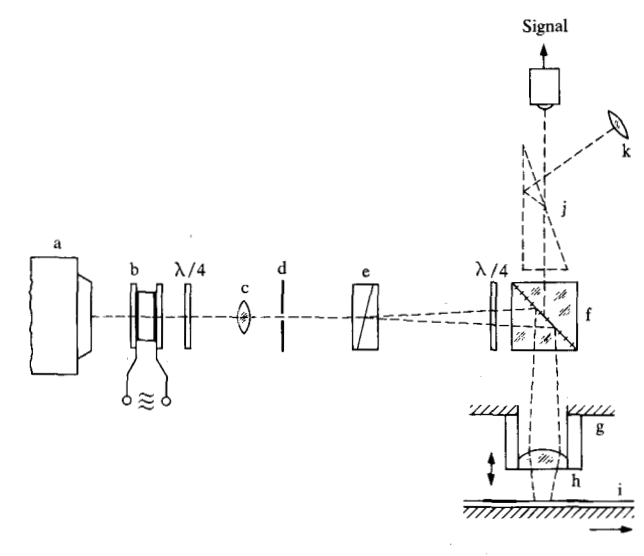
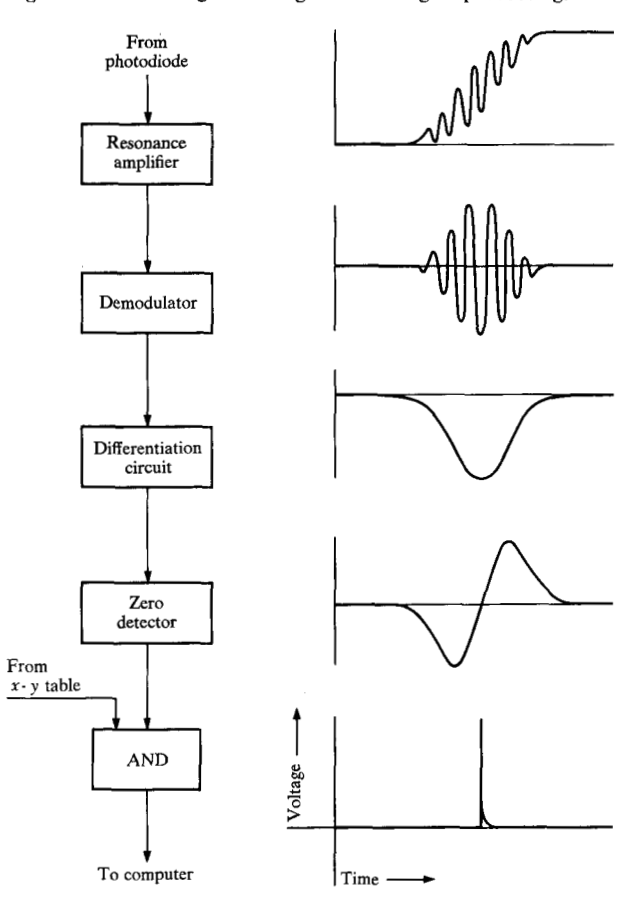
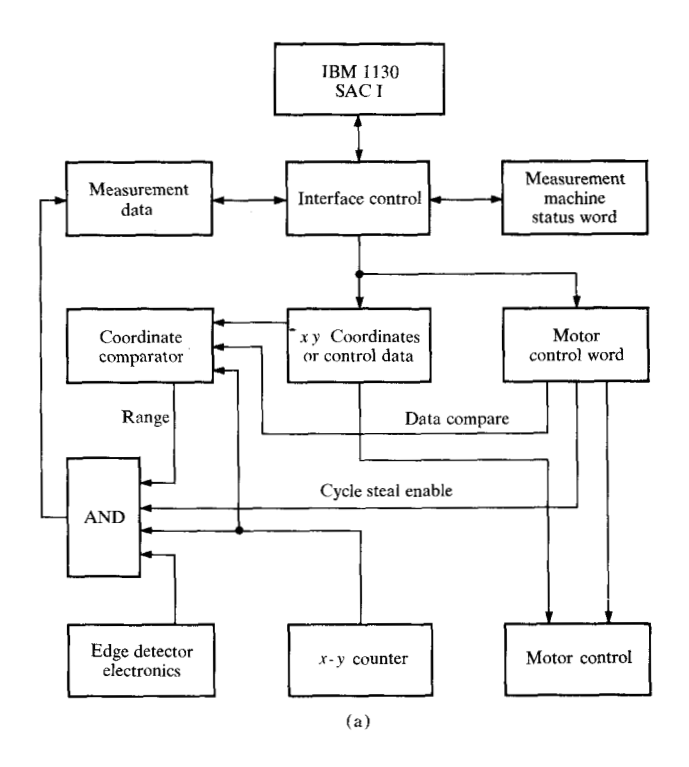


Figure 3 Schematic diagram of edge detection head. (a) He-Ne laser; (b) Pockels cell, operated at 2 MHz; (c) lens; (d) spatial filter; (e) Wollaston prism (angle split = 2 arcminutes); (f) beam splitter; (g) piezoelectric translator (range:  $\pm$ 5  $\mu$ m); (h) microscope objective (N.A. = 0.4); (i) chrome mask; (j) insertable deflection prism: (k) eye piece; (l) photodiode. Parallel to (j), a vibrating diffusor (not shown) is swept into the optical path between (e) and (f), providing granulation-free illumination of the field of view at a safe intensity level.

Figure 4 Block diagram of edge detector signal processing.





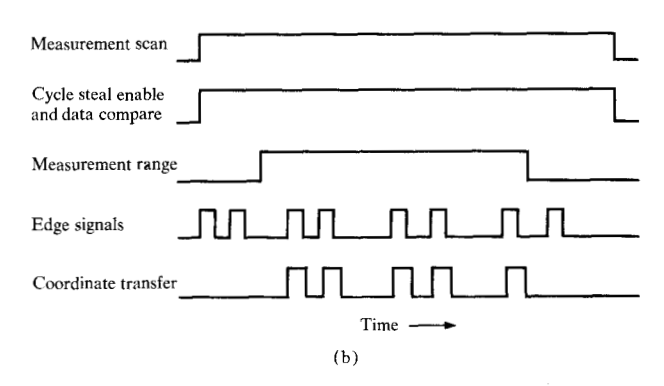


Figure 5 System for interface control. (a) System configuration and (b) signal sequence.

with an automatic refocusing arrangement. The servo movement of the lens is achieved by a piezoelectric translator, and the lens-to-mask distance is monitored by a pair of pneumatic nozzles. The dynamic range of the piezotranslator is  $\pm 5~\mu m$ , which turns out to be sufficient if the mask fixture has been manually preleveled.

#### Environment

In comparison with the environment in which most highprecision measurement equipment is used, the present system is under adverse conditions, both from the mechanical and the climatic point of view. The measurement room is installed on the second floor of a building, and nearby laboratory areas include heavy equipment that excites building vibrations when in operation. The measurement room itself is air conditioned, but without temperature stabilization. The computer, including the peripheral equipment, is installed in the same room with the measuring equipment.

To reduce the interference of mechanical vibrations, the x-y table, interferometer, and edge detector platform are mounted on a rigid, cast-iron base plate. This plate in turn rests on an isolation pad of styrofoam 30 cm thick.

Consideration of the influence of sample and system temperatures is of fundamental importance for any precision measurement system. In an interferometric system the effective laser wavelength is also influenced by air temperature, air pressure, and humidity. In the present system these influences are compensated for by frequent measurements of all parameters and subsequent numerical data correction. At the same time, care is taken that the parameters vary slowly in terms of the average measuring time per problem. For this purpose, the x-y table and dual-axis interferometers are placed in a plexiglass box that shields the interferometers against air turbulence and convection. The main heat sources-the laser and the x-axis stepping motor—are located outside the box. Instruments are provided to monitor the temperature of the sample as well as the temperature, barometric pressure, and humidity of the atmosphere inside the box. The sample temperature is measured by an electronic thermometer to within 10<sup>-2</sup> °C. The sensor is mounted in the vacuum chuck close to its surface, which is in contact with the sample.

All instruments are read at the beginning and end of each measuring period, the mean value being used for data correction. Using a constant value can be considered legitimate, since the duration of a measuring period does not exceed 10 to 20 minutes. The basis for the numerical correction is the dependence of the interferometer step width  $(\lambda/8)$  on temperature t, total pressure p, and relative humidity  $\varphi$  of air according to the expression recently given by Popela [10]:

$$\lambda/8 = 79.100000 + \Delta\lambda,$$

$$\Delta\lambda = (0.095pt - 0.05t - 30.2p + 0.05\varphi t - 0.215\varphi + 23936) \times 10^{-6},$$

where  $\lambda$  and  $\Delta\lambda$  are given in nm, t in  ${}^{\circ}$ C, p in Torr, and  $\varphi$  in percent.

## • Computer control and data acquisition

#### Computer configuration

The computer system consists of an IBM 1131D central processing unit with an internal storage capacity of 32K words (16 bits per word). In addition, the CPU has a

single disk storage with a capacity of 512K words; CPU cycle time is 2.2  $\mu$ s. For input/output purposes an IBM 1442 card reader punch unit and an IBM 1132 printer are provided. The measuring system is connected to the CPU via the storage access channel (SAC I) and a specially designed interface unit.

#### System interface

This unit is designed to control data transfer between the computer and the measuring system. Control information and data are stored in a number of registers that are addressed by the interface control (see Fig. 5). The conditions of the measuring system are sensed in a measuring machine status word, which indicates the type of the required data transfer to the interface control. The motor control word and control data register control the movement of the x-y table and the measurement range. The control data register serves two purposes. In the index or positioning mode it contains the x-y coordinates for the table, whereas in the scanning mode it holds the two limits of the measuring range.

In the scanning or measuring mode the motor control word provides the signals "cycle steal enable" and "data compare." The latter controls the comparison of the control data register with the x-y counter and thereby activates the transfer of the x-y coordinates from the x-y counters into the measurement data register.

The x-y coordinates are read in parallel into the measurement data register 700 ns after the least significant bit of the counters has changed. After the transfer a cycle steal request (CSREQ) is made and the four-word content of the register is moved serially into the core memory of the CPU. The transfer is done during the cycle time of the CPU  $(2.2 \ \mu s)$ . Therefore the total transfer time of the coordinates for one measurement point is

700 ns + CSREQ time + 
$$(4 \times 2.2) \mu s \approx 12 \mu s$$
.

Correspondingly, the maximum rate of measurement is 80 000 points per second.

## Data acquisition

The operation sequence of the measurement data acquisition is shown in Fig. 6. The main program is written in FORTRAN using assembler subroutines. At the beginning of any measurement program the motor control words and the control data, i.e., the x-y coordinates and the upper and lower limits of the measurement range, are read from punched cards into the CPU. The control data, which are eight digits per coordinate, are decoded from the punched card code into the BCD code.

Table coordinates and motor control words are then read into the interface registers. The table is indexed to the first scan position. A new motor control word and the limits of the measurement range are read into the

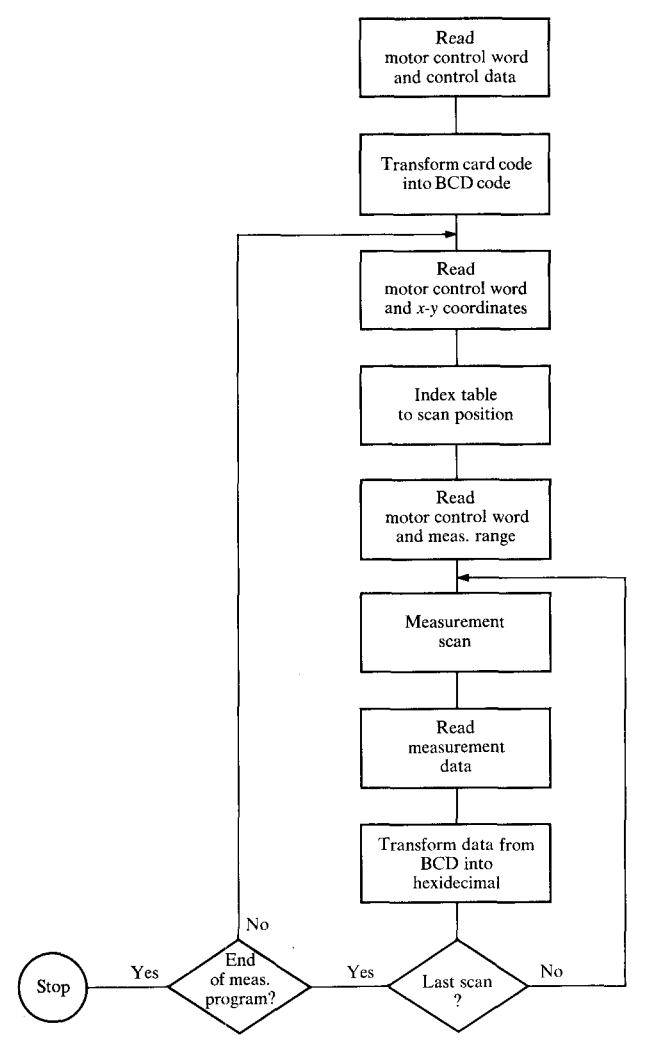


Figure 6 Operation sequence of measurement data acquisition.

control data register. During the table scan all measurement data are read into the CPU main storage. These data are relocated after the scan from the main-storage area into the disk storage area. Multiple scans in the y-direction can be performed with y being either different or constant for all scans. The latter means a repeated measurement along the same trace and thereby improves the measurement precision.

Up to 5000 x-y coordinates (20K words) can be stored in the CPU main storage per individual scan. Even this storage capacity is not sufficient if an actual integrated circuit pattern area is to be scanned completely. In this case the measurement range has to be subdivided into a number of smaller ranges which select the areas of interest and suppress all other data.

For data manipulation in the computer all measurement data that are stored in the BCD form are trans-

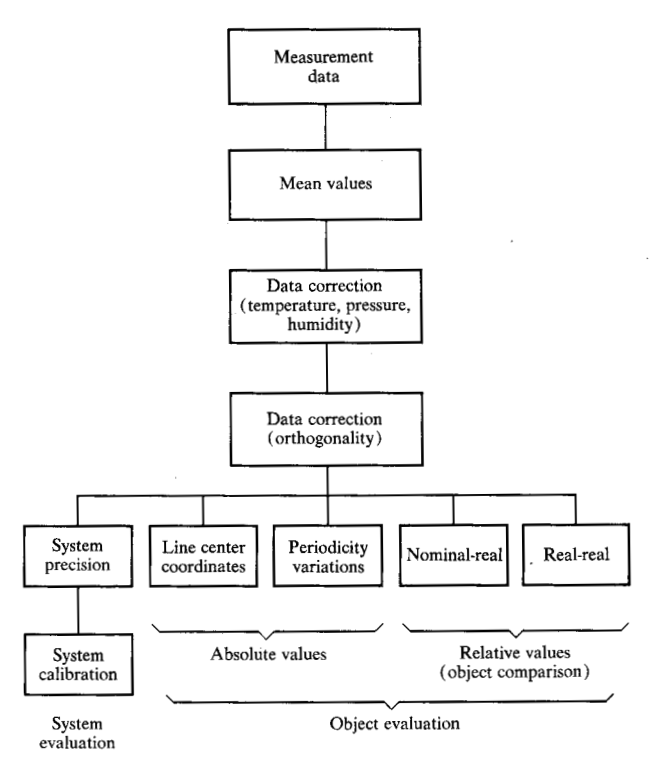
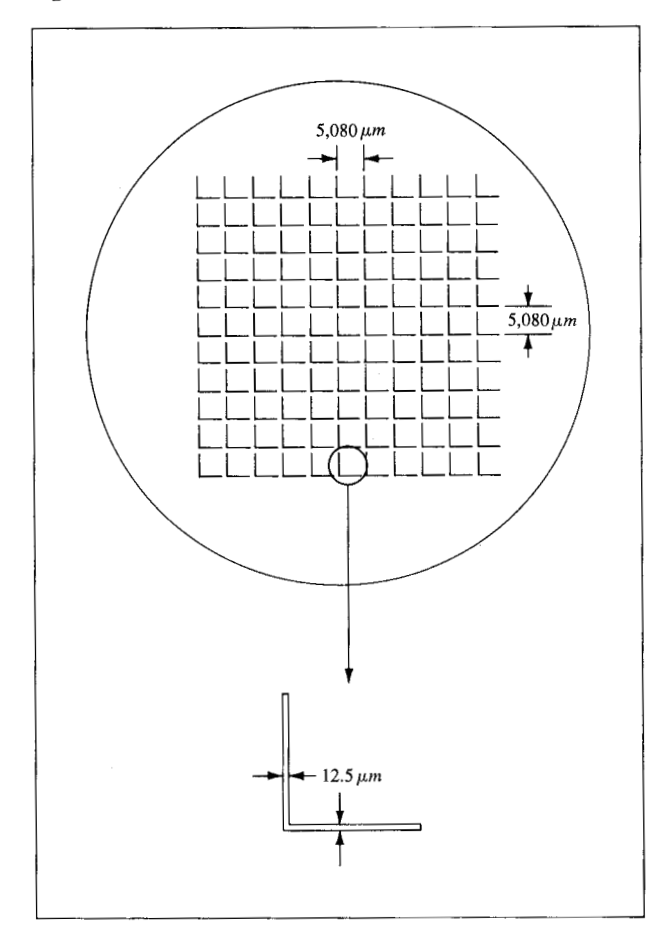


Figure 7 System permitting various data evaluation programs.

Figure 8 Test mask pattern.



formed into the hexadecimal code. This transformation is done after the completion of each measurement program.

## Data evaluation

A program has been written that permits the data to be manipulated in a number of different ways. Various subroutines can be selected through the CPU keyboard switches. Figure 7 shows in block diagram form the possible data evaluation schemes.\*

The measurement data usually stored on the single disk storage are read into the main storage. If there are any multiple scans from the same object site the arithmetic mean value of these data is determined. Thereafter, these data are corrected for environmental deviations that have been recorded during the measurement period. If real two dimensional measurements have been made, the error in orthogonality is determined and the data are corrected for the measuring system error.

For system evaluation various statistical operations have been programmed, and data distributions can be printed, with mean values and maximum deviations.

The object can be evaluated either against itself or against a standard or another object. In the first case deviations from mean values such as linewidth or periodicity are calculated and printed. Either line center coordinates or edge coordinates may be used. In the second case the standard data are read from a card file onto the disk and the comparison is made from the disk file. All evaluations can be made with the data either in multiples of  $\lambda/8$  (smallest count from the interferometer) or in increments of  $10^{-2} \mu m$ . Data output is in printed form and/or as punched cards.

#### System evaluation

The capabilities of the measuring system have been tested in a number of experiments. Since measurement accuracy is a matter of calibration, the main effort has been to determine the measurement precision or repeatability of the complete system. An experiment is described here that shows the short- and long-term stability of the system.

The measurement object was a simple L-shaped chrome pattern (Fig. 8) replicated on a glass plate in an  $11 \times 11$  array. The glass plate dimensions were 100 mm  $\times$  100 mm  $\times$  1.6 mm with a chrome layer thickness of about 100 nm. The thermal expansion coefficient of the glass plate was determined experimentally to be  $8.33 \times 10^{-6}$  °C<sup>-1</sup>. To determine the measurement repeatability, one column of the pattern array was repetitively measured. These measurements were carried out in one dimension only. The pattern coordinates were recorded

<sup>\*</sup>The various programs mentioned here were developed for experimental use on this project and are not available for external distribution.

	Y-mean	Y-max	Y-min	Y-dif	X-mean	X-max	X-min	X-dif
1	495184.9	495178.	495191.	13.	0.0	0.	0.	0•
2	495185.2	495179.	495192.	13.	159.1	160.	158.	2.
3	495263.1	495256.	495268.	12.	64230.1	64231.	64229.	2•
4	495263.0	495256.	495268.	12.	64389.2	64391.	64388.	3.
5	495340.4	495334.	495347.	13.	128451 1	128452.	128450.	2•
6	495340.2	495334.	495346.	12.	128609.6	128611.	128608.	3∙
7	495418.3	495412.	495424.	12.	192675•5	192677.	192675.	2•
8	495418.0	495411.	495424.	13.	192835•1	192836.	192834.	2•
9	495496 2	495490.	495501.	11.	256898•6	256900•	256898.	2•
10	495495.5	495489.	495501	12.	257058•6	257060.	257058.	2•
11	495573.7	495567.	495580.	13.	321127.2	321128.	321126.	2•
12	495573.0	495567.	495579.	12.	321286.5	321288.	321286.	2•
13	495652.4	495647.	495658.	11.	385354.5	385356.	385354•	2.
14	495651.7	495646.	495657.	11.	385513.0	385514.	385512.	2•
15	495729.1	495723.	495735.	12.	449581.6	449583.	449581.	2•
16	495728.5	495723.	495734.	11.	449739.1	449740	449738.	2•
17	495807.2	495800 •	495813.	13.	513808•0	513809.	513807.	2•
18	495806.6	495799.	495913.	14.	513966.4	513968.	513965.	3.
19	495884.7	495878.	495890	12.	578031.9	578033.	578031.	2.
20	495884.2	495877.	495890.	13.	578190.8	578192.	578190.	2.
21	495962.6	495955.	495967.	12.	642255.9	642257.	642255.	2.
22	495962.1	495955.	495966.	11.	642414.7	642416.	642414.	2•

Figure 9 Print-out of edge coordinates in units of  $\lambda/8 = 0.079 \ \mu m$ .

in the x dimension, whereas the y dimension monitored the table movement perpendicular to the scanning direction. Seventy-two measurement trials were carried out during a one-month interval to determine the long-term precision. Each trial consisted of 39 measurements made in a row within a total measurement time of 12 minutes. The evaluation of these individual trials gives the short-term precision. With the 11 lines, or 22 edges per column, and the 39 repetitions, each trial consisted of 858 measured coordinate points. The total data base for the long-term stability is  $72 \times 858 = 61,776$  measurement points.

All measurements were made in an uncontrolled environment. However, the environmental parameters were recorded and the measurement data corrected based on the known linear expansion coefficient of the mask and Popela's expression for the interferometer increment. The analysis that follows is based on data so corrected. During the complete experiment the ranges of variation were about 19° to 24°C for the mask and air temperatures, respectively; 699 to 732 Torr for the barometric pressure; and 10 to 30 percent for the relative humidity. The accuracies of the instruments used were 0.03°C for the mask thermometer, 0.05°C for the air thermometer, and 0.2 Torr for the barometers.

#### Data analysis

The measurement data are evaluated with the assumption that the measurement precision is determined by a short-term and a long-term portion and that each measurement point can be represented by  $X_{jr} = \mu + \delta_r + \epsilon_{jr}$ , where  $\mu$  represents the real pattern coordinate, and  $\delta_r$  is

the long-term and  $\epsilon_{jr}$  the short-term portion of the measurement deviation. The quantities j and r are the number of repetitions of the measurement and of the trial, respectively.

The total precision of the measuring system for line center coordinate measurement can be described by the standard deviation

$$\sigma_{t} = [p^{-1} \sigma_{s}^{2} + (np)^{-1} \sigma_{s}^{2}]^{\frac{1}{2}}$$

for p trials and n measurements per trial. Normal distributions of the different groups of data are assumed for this analysis. This hypothesis has been proved by appropriate statistical tests.

#### Short-term precision

Short-term precision of the system is obtained from the data evaluation of each measurement trial. To eliminate the influence of temperature variations on the mechanical stability of the setup, all measurements are referenced to the mask coordinate system rather than to that of the measuring system. This is achieved by subtracting the *x* coordinate of the first edge from all the following ones:

$$X_i = X_i' - X_i'$$
  $1 \le i \le k$   $(k = 22)$ 

in which i is the index of the edge location.

From the 39 measurement values obtained in each trial a mean value

$$\overline{X}_i = \frac{1}{n} \sum_{i=1}^n X_{ij} \qquad 1 \le j \le n \qquad (n = 39)$$

has been determined for each edge coordinate.

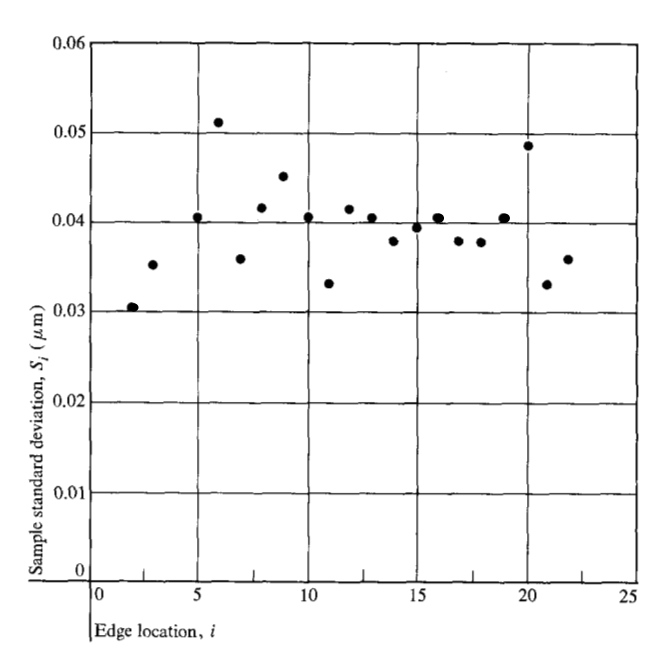


Figure 10 Sample standard deviation  $S_i$  vs the index i of edge location.

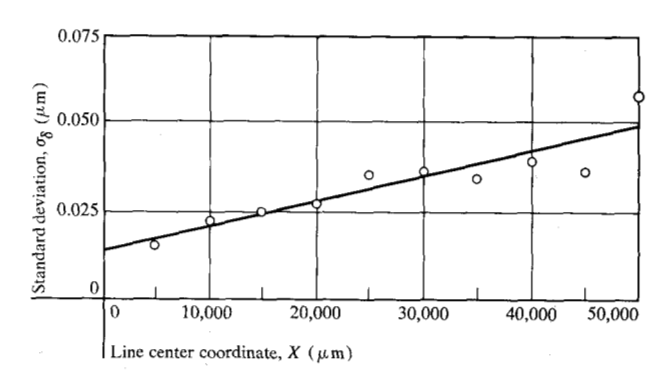


Figure 11 Long-term precision  $\sigma_{s}$  vs X.

Figure 9 is a printout of the mean coordinates  $\overline{X}_i$  and  $\overline{Y}_i$  for one trial. Also the two extreme values measured during the trial, together with the ranges of measurement deviation, are given in the printout. All data are in multiples of  $\lambda/8$  (= 0.08  $\mu$ m), the least count of the interferometers.

Figure 9 shows that the table error, indicated by the variation of the y coordinate, is  $\pm 6$  digits. The measurement repeatability given by the measurement range in the x coordinate is  $\pm 1.5$  digits.

A statistical analysis of the data has been carried out to determine the trial variances and standard deviations to obtain a more predictable result. The sample variance of the  $X_{ii}$  was calculated according to

$$S_i^2 = \frac{1}{n-1} \sum_{j=1}^n (X_{ij} - \overline{X}_i)^2 - \frac{\Delta X^2}{12}.$$

The second part of this expression is Sheppard's correction [11] for the digitizing error that occurs because of the finite resolution  $\Delta X$  of the interferometer.

Figure 10 shows the distribution of the sample standard deviations  $S_i$  over the edge locations for an arbitrary trial. These data show no significant dependency on location. This means that the reduction in measurement time has in fact eliminated any significant time-dependent measurement deviations. Therefore, a mean value can be calculated to describe the variance of each measurement trial

$$S_r^2 = \frac{1}{k} \sum_{i=1}^k S_i^2$$
  $1 \le r \le p$   $(p = 72).$ 

The  $S_r^2$  vary slightly as a function of the trials, but here, too, no time dependency can be deduced. Because of the sample size, the sample variance  $S^2$  and the total population variance  $\sigma^2$  are about the same. Therefore, a total standard deviation involving all available data can be determined as

$$\sigma_{\epsilon} = \left(\frac{1}{p} \sum_{r=1}^{p} S_r^2\right)^{\frac{1}{2}} = 0.038 \ \mu \text{m}.$$

This value is the short-term standard deviation of the measurement system. It represents all short-term variations during the measurement, such as electrical and mechanical noise in the various parts of the system.

#### Long-term precision

For the determination of the short-term precision, all 72 trials have been assumed to be independent, and only the deviations of the measured values  $X_{ij}$  from their individual mean values  $\overline{X_i}$  have been evaluated. For the long-term precision analysis the deviations of the  $\overline{X_i}$  from a common mean value over the 72 trials have been calculated. To reduce the amount of data the line center coordinates  $X_i$  have been used instead of the edge coordinates  $X_i$ 

$$X_l = \frac{1}{2} (X_{2l-1} + X_{2l}) \qquad 1 \le l \le m \qquad (m = 11).$$

The mean values of the individual trials  $\overline{X_l}$  and the common mean  $\overline{\overline{X_l}}$  are given by

$$\overline{X}_{l} = \frac{1}{n} \sum_{j=1}^{n} X_{ij},$$

$$\overline{\overline{X}}_{l} = \frac{1}{p} \sum_{r=1}^{p} \overline{X}_{lr}.$$

From these values the sample variance for each line center coordinate can be determined as

$$S_l^2 = \frac{1}{p-1} \sum_{r=1}^p (\overline{X}_{lr} - \overline{\overline{X}}_l)^2.$$

This sample variance represents the combined effect of short- and long-term precision. Subtracting the short-term variance  $S_{\epsilon}^{\ 2}$ , adjusted for the number of measurements, and taking into account the line center coordinate calculation, permits the long-term precision to be written as

$$S_s^2 = S_t^2 - (S_{\epsilon}^2/2n).$$

Again the variance of the total population  $\sigma_{\delta}^2$  is used in the following example instead of the sample variance.

Figure 11 shows the resulting standard deviation  $\sigma_{\delta}$  for the different line center coordinates. Contrary to the results for the short-time precision, in this case there is a dependency on the measurement range with the assumption that this relation is linear, a regression analysis leads to the expression

$$\sigma_8 = 7 \times 10^{-7} X + 0.015 \ \mu \text{m}.$$

This value represents all long-term variations of the system that are mainly due to environmental changes. In addition it includes the variations introduced by the handling and alignment of the mask.

#### Conclusions

An experimental measuring system has been built and evaluated which permits geometrical measurements at high speed with a precision comparable to that of to-day's slower measuring machines. The system can measure the two-dimensional geometry of integrated circuit patterns with an area up to  $100~\text{mm} \times 100~\text{mm}$ . Pattern widths and spacings down to  $2~\mu\text{m}$  within a topography range of  $10~\mu\text{m}$  can be determined.

The major components that have been developed are the coplanar *x-y* interferometer and the high-speed edge detection microscope. These components, together with the IBM 1130, give the speed and precision required.

The new approach in geometrical measurement has been successfully tested. In particular the result of the short-term analysis, which gave a standard deviation  $\sigma_{\epsilon}=0.038~\mu m$ , shows that the high measurement speed practically eliminates the influence of the environmental changes and other slowly varying parameters. Even the influence of mechanical vibrations has been reduced to an insignificant level, thereby eliminating the need for the heavy foundations usually required for high-precision measuring machines. Environmental changes can be tolerated over a much larger range provided the variations are recorded and the data corrected. The statistical tests that have been carried out show with sufficient sig-

nificance that the precision of the instrument can be described by a short-term part  $\sigma_{\epsilon}$  independent of the measurement range, and a long-term part  $\sigma_{\delta}$  with a range dependence. However, the total analysis was somewhat handicapped by the limits of resolution of the interferometric measuring system. As Fig. 9 indicates, only a maximum of four classes are occupied by the measured values, and statistics with such a small distribution are not too accurate. Therefore, the numerical values obtained for the measurement precision will be on the high side. To obtain more accurate results the resolution has to be increased. Plans are being developed to use  $\lambda/16$  increments instead of  $\lambda/8$  increments.

Further work is also to be carried out in the longterm precision analysis. In order to obtain the right interval for recalibration, the change of long-term precision with time has to be determined.

As already noted, the present analysis refers essentially to one-dimensional measurements along parallel traces in the x-direction. Future work will be aimed for a similar analysis for true two-dimensional operation. The full knowledge of pattern geometries in two dimensions will be increasing in importance, because manufacturing tolerances tend to decrease for all new technologies.

#### References

- A. W. Young, Proceedings of MICROTECNIC 1973, Edition Microtecnic Scriptar SA, Avenue de la Gare 23. CH-1003 Lausanne, Switzerland.
- 2. G. W. Stroke, Encyclopedia of Physics, 29, 426 (1967).
- G. R. Harrison and S. W. Thompson, J. Opt. Soc. Am. 60, 591 (1970).
- (a) F. Hock and K. Heinecke, Maschinenmarkt 71, 27 (1965); (b) M. R. Radio et al, IBM J. Res. Develop. 14, 641 (1970).
- 5. A. Weyrauch, Optik 28, 242 (1968).
- P. Fretwell, Proceedings of MICROTECNIC 1973, Edition Microtecnic Scriptar SA, Avenue de la Gare 23, CH-1003 Lausanne, Switzerland.
- 7. J. Dyson, *Interferometry as a Measuring Tool*, The Machinery Publishing Co., Ltd., Brighton, England 1970.
- 8. F. Schedewie, Israel J. Technol. 9, 263 (1970).
- 9. F. Schedewie, Optik 37, 404 (1973).
- 10. B. Popela, Optica Acta 19, 605 (1972).
- 11. B. L. Van der Waerden. Mathematische Statistik, Springer, Berlin, 1965.

Received March 20, 1973

The authors are located at the German Manufacturing Technology Center, IBM Deutschland GmbH, 7032 Sindelfingen, Germany.